Droop-Control-Based State-of-Charge Balancing Method for Charging and Discharging Process in Autonomous DC Microgrids

Lu, Xiaonan; Sun, Kai; Guerrero, Josep M.; Vasquez, Juan Carlos; Huang, Lipei

Published in:
Proceedings of the IEEE International Symposium on Industrial Electronics, ISIE 2014

DOI (link to publication from Publisher):
10.1109/ISIE.2014.6864988

Publication date:
2014

Document Version
Early version, also known as pre-print

Droop-Control-Based State-of-Charge Balancing Method for Charging and Discharging Process in Autonomous DC Microgrids

Xiaonan Lu[1], *Student Member, IEEE*, Kai Sun[2], *Member, IEEE*, Josep M. Guerrero[3], *Senior Member, IEEE*, Juan C. Vasquez[3], *Member, IEEE*, Lipei Huang[2]

1. Department of Electrical Engineering & Computer Science, University of Tennessee, Knoxville, TN 37909, US
2. Department of Electrical Engineering, Tsinghua University, Beijing, 100084, China
3. Department of Energy Technology, Aalborg University, Aalborg East, 9220, Denmark

***Abstract*—In this paper, a droop control based state-of-charge (SoC) balancing method in autonomous DC microgrids is proposed. Both charging and discharging process have been considered. In particular, in the charging process, the droop coefficient is set to be proportional to SoC^n, and in the discharging process, the droop coefficient is set to be inversely proportional to SoC^n. Since the injected/output power is in inverse-proportion to the droop coefficient, with the proposed method, the energy storage unit (ESU) with higher SoC absorbs less power in the charging process and delivers more power in the discharging process. Meanwhile, the ESU with lower SoC absorbs more power in the charging process and delivers less power in the discharging process. Eventually, the SoC and injected/output power in each ESU are equalized. The exponent n for SoC is employed to regulate the balancing speed of the SoC and injected/output power. It is demonstrated that with higher exponent n, the balancing speed is higher. Simulation model comprised of three ESUs is implemented by using MATLAB/Simulink. The proposed method is verified by the simulation results.**

Keywords — distributed energy storage unit; droop control; dc microgrid; state-of-charge

I. INTRODUCTION

With the development of modern electric grid, sustainable energy has gained more awareness nowadays. At the same time, in order to electrify the remote area and efficiently integrate different kinds of renewable energy sources, the concept of microgrid was proposed several years ago [1] and has been intensively studied in the recent years [2]-[14]. Since the conventional electric grid is implemented based on ac system, ac microgrids have drawn more attention [2]-[7]. However, various sources and loads in a microgrid have dc couplings, e.g. photovoltaic (PV) panels, batteries, LEDs, etc. Hence, it is a simpler and more efficient way to connected them with dc-dc converters to form a dc microgrid. In contrast to ac microgrids, dc microgrids do not have the problems caused by harmonics and reactive power, and can operate with higher efficiency [8]. Considering the above advantages, there is an increasing research interests on dc microgrids recently [9]-[14].

In order to connect the renewable energy sources and the loads to the point of common coupling (PCC), power electronics converters are usually employed as the interfaces [15]. Power sharing between different interfacing converters is a key problem in the control system of microgrids [1]-[7], [9], [11]-[14]. Different approaches have been proposed in the literatures, e.g. master-slave control [16], 3C control [17], average current control [18], droop control [1]-[7], [9], [11]-[14], etc. Since the sources and loads are connected to the common bus dispersedly, droop control and its variants as decentralized methods have been widely studied [1]-[7], [9], [11]-[14]. In a dc microgrid, droop control is achieved by linearly reducing the dc voltage reference value as the load increases, and vice versa. Hence, the output power of each interfacing converters can be automatically equalized by regulating the dc output voltage.

Although renewable energy sources have many advantages, their output power possesses the stochastic and intermittent properties. In order to solve these problems, the energy storage units (ESUs) should be employed to restrain the power fluctuation [19]. Considering the distributed connection of the sources and loads in a microgrid, distributed energy storage units (DESUs) are commonly used. An ESU is usually formed by series connected battery cells, and the string of battery cells is connected to the common bus. Hence, the control system of the ESUs is comprised of two parts. They are battery management system (BMS) and power converter system (PCS), respectively [14]. The function of BMS is to monitor the state of each battery unit in an ESU, and to balance the state-of-charge (SoC) of each unit. The function of PCS is to control the output voltage and current, and also to reach the proper load power sharing. In order to efficiently use the DESUs and prolong their life, two requirements regarding SoC should be satisfied. First, the SoC of each cell in the battery string of an ESU should be balanced. Second, the SoC of the whole ESU should be balanced among different ESU modules. The first

requirement can be achieved by using the BMS, and the second can be achieved by using the PCS.

This paper is a continuous work of [14]. Aiming at PCS, the decentralized control system based on droop control is developed to balance the SoC of each ESU and equalize the injected/output power of each corresponding interfacing converters. In [14], only the discharging process is studied. Here, double-quadrant operation modes are under consideration. In particular, in the charging operation mode, the droop coefficient is set to be proportional to the n^{th} order of SoC. Since the injected power of the interfacing converter for the ESU is inversely proportional to the droop coefficient, the injected power can be inversely proportional to the n^{th} order of SoC. It means that the ESU with higher SoC is charged with less power, while the ESU with lower SoC is charged with more power. Hence, the SoC can be gradually balanced, and the injected power of each ESU is thereby equalized. In the discharging operation mode, the droop coefficient is set to be inversely proportional to the n^{th} order of SoC. Since the output power is also inversely proportional to the droop coefficient, the output power is set to be proportional to the n^{th} order of SoC. It means that the ESU with higher SoC delivers more power, while the ESU with lower SoC delivers less power. As same as the condition in the charging mode, the SoC of each ESU can be gradually balanced, and the output power is equalized. It should be noticed that the exponent n is employed in the above method to regulate the power sharing speed. It can be demonstrated that with larger exponent n, the SoC balancing and power sharing speed is enhanced.

II. Double-quadrant SoC-based Droop Control Methods

A. Principle of the proposed method

The configuration of the autonomous dc microgrid is shown in Fig. 1, which is comprised of three parts: (I) sources, (II) loads, and (III) DESUs. Part I is formed by the distributed renewable energy sources, which operate in MPPT mode and inject power into the common bus. Part II is formed by the loads, which absorb power from the common bus. As mentioned above in Section I, considering the stochastic and intermittent property of the sources in Part I and also the load changing in Part II, DESUs should be employed in the dc microgrids, as shown in Part III. When the power generated in Part I is higher than the power consumed in Part II, sufficient power is supplied in the system and the DESUs operate in the charging mode. On the other hand, when the power generated in Part I is lower than the power consumed in Part II, the power in the system is not enough to feed the loads. Hence, the DESUs operate in the discharging mode to match the power difference.

As aforementioned, the charging and discharging operation modes with SoC balancing and inject/output power equalization are the efficient status to guarantee the reliable operation of the DESUs. Considering the decentralized configuration of the ESUs in dc microgrids, droop control as a kind of distributed control method is selected as the basis of the proposed method. The conventional droop curve in the first quadrant can be extended to obtain the double-quadrant droop curve, as shown in Fig. 2. The part of the droop curve in the first quadrant represents the discharging process, and the part in the second quadrant represents the charging process. It is seen in Fig. 2 that in the charging mode, with higher droop coefficient the injected power is lower, and with lower droop coefficient the injected power is higher. In the discharging mode, with higher droop coefficient the output power is lower, and with lower droop coefficient the output power is higher.

The expression of droop control in dc microgrids can be shown as:

$$v_{dci}^{*} = v_{dc}^{*} - m_i \cdot P_{oi} \tag{1}$$

where v_{dci}^{*}, m_i and P_{oi} are the reference of dc output voltage, droop coefficient and filtered power by the low-pass filter (LPF) of converter #i respectively, v_{dc}^{*} is the reference of dc output voltage at no-load condition (i = 1, 2, … , k, and k is the number of the ESUs in the dc microgrid).

It should be noticed that P_{oi} is positive in the discharging process, while it is negative in the charging process.

In order to meet the requirement of SoC balancing, in the charging operation mode, the droop coefficient is set:

$$m_i = m_c \cdot SoC_i^n \tag{2}$$

where m_c is the droop coefficient for charging process when the ESU is fully charged, n is the exponent of SoC which is involved to regulate the speed of SoC balancing.

The IEC-60228 has shown the line resistance of the power cable [20]. It can be found that for the power cable whose cross-sectional area is larger than 8 cm^2, the line resistance is less than 0.04 Ω/km. Assuming that the voltage level of the system is 600 V, when the power of 1 kW flows through the power cable of 1 km, the voltage drop across the line is less than 0.067 V, which is much smaller than nominal voltage level of the system. Hence, the voltage drop across the power cable can be neglected. Therefore, it yields:

$$v_{dc1} \approx v_{dc2} \approx \cdots \approx v_{dck} \tag{3}$$

Considering the ideal voltage controller is used, the actual dc output voltage is equal to its reference value. Combining (1) – (3), it is derived:

$$P_{o1} : P_{o2} : \cdots : P_{ok} = \frac{1}{SoC_1^n} : \frac{1}{SoC_2^n} : \cdots : \frac{1}{SoC_k^n} \tag{4}$$

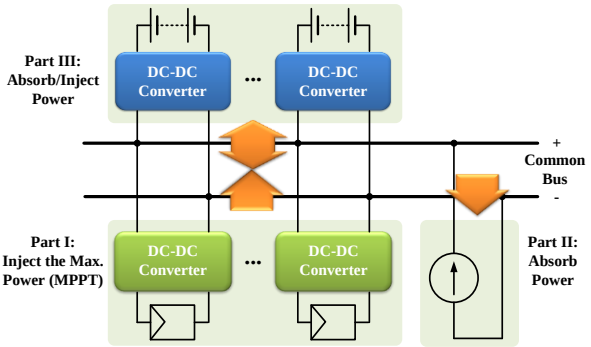

Fig. 1. The configuration of the autonomous dc microgrid.

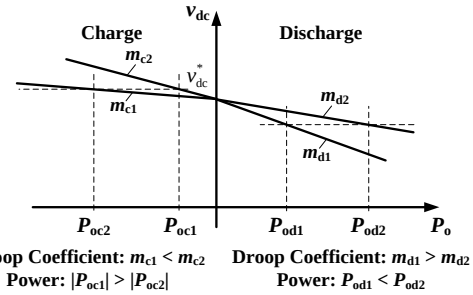

Fig. 2. Curve of the double-quadrant droop control.

It is concluded from (4) that in the charging operation mode, if $SoC_i > SoC_j$ (i, j = 1, 2, … , k), then $|P_{oi}| < |P_{oj}|$. It means that the increasing speed of SoC_i is lower than SoC_j. Hence, SoC_i and SoC_j are gradually balanced. Meanwhile, the injected power P_i and P_j are thereby equalized.

In the discharging operation mode, the droop coefficient is set:

$$m_i = \frac{m_d}{SoC_i^n} \tag{5}$$

where m_d is the droop coefficient for discharging process when the ESU is fully charged, n is the exponent of SoC which is involved to regulate the speed of SoC balancing.

As same as the condition in the charging process, the voltage drop across the power line can be neglected. Therefore, the expression in (3) is also satisfied. Combining (1), (3) and (5), it is reached:

$$P_{o1} : P_{o2} : \cdots : P_{ok} = SoC_1^n : SoC_2^n : \cdots : SoC_k^n \tag{6}$$

It is concluded from (6) that in the discharging operation mode, if $SoC_i > SoC_j$ (i, j = 1, 2, … , k), then $P_{oi} > P_{oj}$. It means that decreasing speed of SoC_i is higher than SoC_j. Hence, SoC_i and SoC_j are gradually balanced. Meanwhile, the output power of ESU #i and ESU #j is equalized.

Assuming the coulomb counting method is used to obtain the SoC of each ESU, the method can be shown below:

$$SoC_i = SoC_{i\,t=0} - \frac{1}{C_{ei}} \int i_{oei} \mathrm{d}t \tag{7}$$

where $SoC_{i\,t=0}$ is the initial SoC_i at the starting time, C_{ei} and i_{oei} are the capacity and output current of the ESU #i.

Meanwhile, considering the power balancing in the input side and output side of the interfacing converter, it yields:

$$p_{oi} \approx p_{oei} = v_{oei} i_{oei} \tag{8}$$

where p_{oi} is the injected/output power of converter #i without low-pass filtering, p_{oei}, v_{oei} and i_{oei} are the injected/output power, voltage and current of ESU #i.

Since the output voltage of the ESU almost keeps constant in a large range of SoC, it is assumed that v_{oei} is a constant value in (8). Hence, combining (7) and (8), it is derived:

$$SoC_i = SoC_{i\,t=0} - \frac{1}{C_{ei} v_{oei}} \int p_{oi} \mathrm{d}t \tag{9}$$

Meanwhile, since the injected/output power changes slowly, the real power (p_{oi}) and the power after the LPF (P_{oi}) are almost the same. Considering the power matching in the system, it is reached:

$$P_{req} = P_s - P_{load} = \sum_{r=1}^{k} p_{or} \approx \sum_{r=1}^{k} P_{or} \tag{10}$$

where P_{req} is the required power in the system which is equal to the difference of the total power supplied by the sources (P_s) and the total power needed by the loads (P_{load}).

Combining (9) – (10) and the proportion shown in (4) and (6), it yields that in the charging operation mode,

$$SoC_i = SoC_{i\,t=0} - \frac{P_{req}}{C_{ei} v_{oei}} \int \frac{\dfrac{1}{SoC_i^n}}{\displaystyle\sum_{r=1}^{k} \frac{1}{SoC_r^n}} \mathrm{d}t \tag{11}$$

In the discharging operation mode,

$$SoC_i = SoC_{i\,t=0} - \frac{P_{req}}{C_{ei} v_{oei}} \int \frac{SoC_i^n}{\displaystyle\sum_{r=1}^{k} SoC_r^n} \mathrm{d}t \tag{12}$$

Take the distributed energy storage system (DESS) with three ESUs as an example. By solving the sets of the equations (10) and (11), the numeric solutions of SoC and injected power in the charging operation mode can be obtained, as shown in Fig. 3. Meanwhile, by solving the sets of equations (10) and (12), the numeric solutions of SoC and output power in the discharging operation modes can be obtained, as shown in Fig. 4. The system parameters are shown in Table I. Here, the exponent n is selected as 6 as an example. It is seen in Fig. 3 and 4 that the SoC and injected/output power of each ESU gradually becomes equal respectively.

B. Speed regulation of the SoC balancing and injected/output power equalization

As mentioned in Section I, the exponent n is employed in the proposed control method to reach the speed regulation of the SoC balancing and injected/output power equalization. Here, two variables $\varepsilon_{soc\,T}$ and $\varepsilon_{po\,T}$ are involved, which are used to define the error of SoC and injected/output power after the time period T. The variables satisfy the following expressions:

$$\varepsilon_{soc\,T} = \left| \max_{i = 1, 2, \ldots, k} \{SoC_{i\,t=T}\} - \min_{i = 1, 2, \ldots, k} \{SoC_{i\,t=T}\} \right| \tag{13}$$

$$\varepsilon_{po\,T} = \left| \max_{i = 1, 2, \ldots, k} \{p_{oi\,t=T}\} - \min_{i = 1, 2, \ldots, k} \{p_{oi\,t=T}\} \right| \tag{14}$$

where $SoC_{i\ t=T}$ and $p_{oi\ t=T}$ are the SoC and injected/output power when $t = T$.

Also take the DESS with three ESUs as an example. By using the same parameters in Table I, the SoC and injected/output power with different exponent n is shown in Fig. 5 and 6. It is found that in both charging and discharging modes, when the larger exponent n is selected, the final errors of SoC and output power become smaller after the same time period.

TABLE I System Parameters

Item	Symbol	Value	Unit
Initial SoC_1	$SoC_{1\,t=0}$	90/60	%
Initial SoC_2	$SoC_{2\,t=0}$	80/50	%
Initial SoC_3	$SoC_{3\,t=0}$	70/40	%
Converter Output Voltage	V_o	600	V
Converter Input Voltage	V_{in}	200	V
Load Power	P_{req}	-3/3	kW
Max. Power Rating of Each Converter	p_{max}	2.5	kW

Min. Power Rating of Each Converter	p_{max}	0.2	kW
Max. DC Voltage Deviation	Δv_{dcmax}	12	V
Min. DC Voltage Deviation	Δv_{dcmin}	2	mV

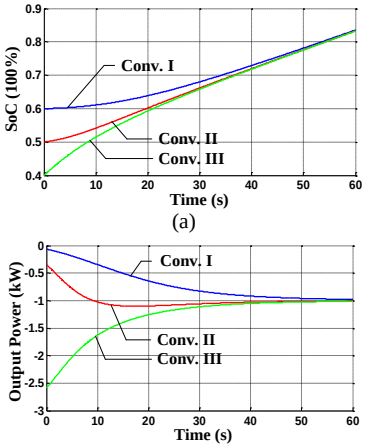

Fig. 3. Waveforms of SoC and injected power in the charging operation mode (n = 6). (a) Waveforms of SoC. (b) Waveforms of injected power.

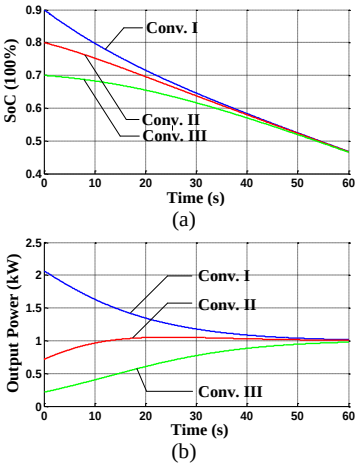

Fig. 4. Waveforms of SoC and output power in the discharging operation mode (n = 6). (a) Waveforms of SoC. (b) Waveforms of output power.

C. Limitations of the parameters used in the control diagram

In the starting period, with larger exponent n, the proportion between different initial SoC^n becomes larger, which results in larger difference in the initial injected/output power. Hence, in order to avoid the unsuitable power which is either too large to exceed the maximum power rating or too small to influence the normal operation of the converter, the exponent n should be limited within the acceptable range. As shown in Fig. 7 (a), in the charging process, the difference of the initial injected power becomes larger. It should be guaranteed that the injected power should not cross the upper and lower boundaries, which are 2.5 kW and 0.2 kW respectively. In the given conditions in Table I, the maximum exponent n should be 6, as marked in Fig. 7 (a). Meanwhile, in the discharging process, the difference of the initial output power also becomes larger with higher exponent n, as shown in Fig. 7 (b). By considering the two boundaries, the maximum exponent n should be 9. Hence, the final upper limit of the exponent n should be selected to meet the requirements in both charging and discharging modes. Concretely, it should be selected to be less than 6.

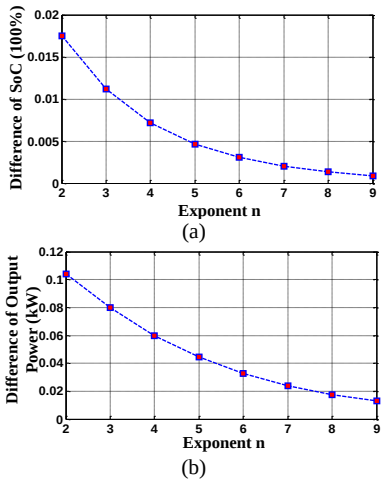

Fig. 5. Final errors of SoC and injected power with different exponent n in the charging operation mode. (a) Final errors of SoC. (b) Final errors of injected power.

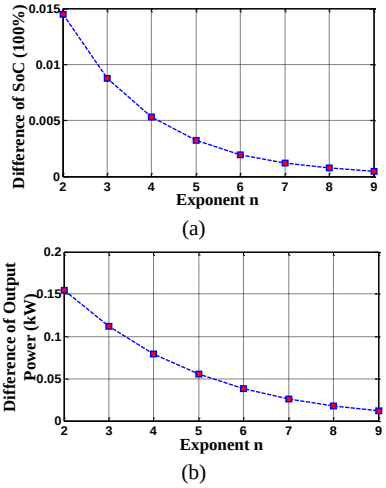

Fig. 6. Final errors of SoC and output power with different exponent n in the discharging operation mode. (a) Final errors of SoC. (b) Final errors of output power.

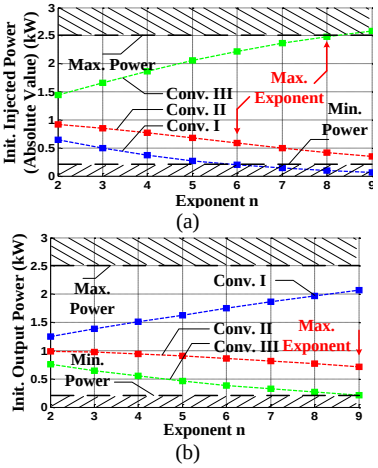

Fig. 7. Initial power with different exponent n in charging process (absolute value). (a) Injected power. (b) Output power.

Another important issue is the dc output voltage. In order to ensure the normal operation of the system, the dc voltage deviation should be neither too large nor too small. If the dc

voltage deviation is too large, the stability of the system cannot be guaranteed. Meanwhile, since droop control works with the dc voltage deviation, if it is too small, the performance of droop control will be influenced. Hence, the following inequalities should be satisfied. Here, the exponent n derived above is used.

In the charging process,

$$\begin{cases} m_c SoC_{max}^n \cdot P_{omax} \le \Delta v_{dcmax} \\ m_c SoC_{min}^n \cdot P_{omin} \ge \Delta v_{dcmin} \end{cases} \quad (15)$$

where SoC_{max} and SoC_{min} are the maximum and minimum values of SoC, P_{omax} and P_{omin} are the maximum and minimum values of injected/output power, Δv_{dcmax} and Δv_{dcmin} are the maximum and minimum values of dc voltage deviation.

In the discharging process,

$$\begin{cases} \dfrac{m_d}{SoC_{min}^n} \cdot P_{omax} \le \Delta v_{dcmax} \\ \dfrac{m_d}{SoC_{max}^n} \cdot P_{omin} \ge \Delta v_{dcmin} \end{cases} \quad (16)$$

Assuming that $35\% \le SoC \le 95\%$ and $0.2\text{ kW} \le P_o \le 2.5\text{ kW}$, (15) and (16) can be solved. It is derived that $5.4\times10^{-3} \le m_c \le 6.5\times10^{-3}$, $7.4\times10^{-6} \le m_d \le 8.8\times10^{-6}$.

III. Simulation Validation

Simulation model comprised of three ESUs is implemented by using MATLAB/Simulink to validate the proposed double-quadrant SoC-based droop control method. Different cases are studied to test the feasibility of the proposed method.

In the charging operation, the waveforms of SoC and injected power when the exponent n equals 2 and 6 are shown in Fig. 8 (a) and 9 (a), respectively. Compared the results in the above two figures, when n equals 2, $\varepsilon_{soc\ T}$ is reduced from 20% to 6%. Meanwhile, when n equals 6, $\varepsilon_{soc\ T}$ is reduced from 20% to almost zero over the same time period. Hence, it is seen that the SoC balancing speed is enhanced in the charging process by increasing the exponent n. The similar results can be found in the waveforms of injected power in Fig. 8 (b) and 9 (b). When n equals 2, $\varepsilon_{po\ T}$ is reduced from 0.8 kW to 0.13 kW. When n equals 6, $\varepsilon_{po\ T}$ is reduced from 2.02 kW to almost zero over the same time period. Hence, the speed of injected power equalization is also enhanced with higher exponent n.

In the discharging operation, when n equals 2 and 6, the waveforms of SoC over the same time period are shown in Fig. 10 (a) and 11 (a), respectively. When n equals 2, $\varepsilon_{soc\ T}$ is reduced from 20% to 4.2%. Meanwhile, when n equals 6, $\varepsilon_{soc\ T}$ is reduced from 20% to almost zero. For the output power, the waveforms over the same time period are shown in Fig. 10 (b) and Fig. 11 (b). When n equals 2, $\varepsilon_{po\ T}$ is reduced from 0.48 kW to 0.23 kW. When n equals 6, $\varepsilon_{po\ T}$ is reduced from 1.35 kW to almost zero. Therefore, it is seen that the speed of SoC balancing and output power equalization is enhanced with higher exponent n.

IV. Conclusion

In this paper, the SoC-based droop control method is proposed to reach the proper power sharing between different ESUs. Both charging and discharging operation modes are taken into account. In the charging process, the droop coefficient is set to be proportional to the SoC^n, while in the discharging process, the droop coefficient is set to be inversely proportional to the SoC^n. It is demonstrated that with the proposed double-quadrant SoC-based droop control method, SoC balancing and injected/output power equalization can be achieved in both charging and discharging modes. The exponent n is employed to adjust the balancing speed. It is found that with higher exponent n, the balancing speed is enhanced. Limits of the parameters in the control scheme are discussed by considering the boundaries employed by the initial power distribution and dc voltage deviation. By selecting the reasonable parameters, the stability of the control system is ensured.

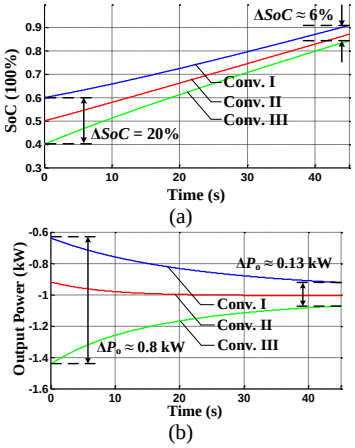

Fig. 8. Waveforms of SoC and injected power in charging mode (n = 2).(a) SoC. (b) Injected power.

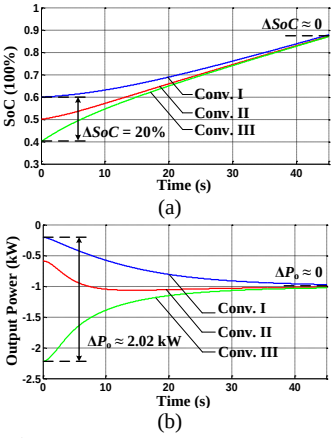

Fig. 9. Waveforms of SoC and injected power in charging mode (n = 6).(a) SoC. (b) Injected power.

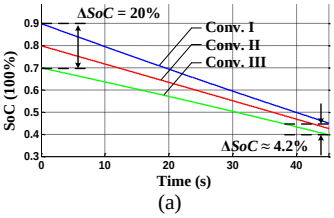

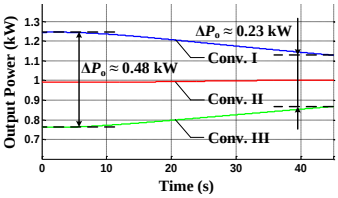

(b)

Fig. 10. Waveforms of SoC and output power in discharging mode (n = 2). (a) SoC. (b) Output power.

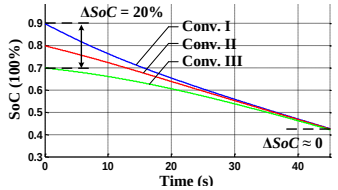

(a)

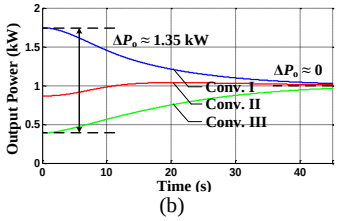

(b)

Fig. 11. Waveforms of SoC and output power in discharging mode (n = 6). (a) SoC. (b) Output power.

ACKNOWLEDGMENT

The authors would like to thank the National Natural Science Foundation of China (51177083) to support the research of this paper.

REFERENCES

[1] R. Lasseter, A. Akhil, C. Marnay, J. Stevens, et al, "The certs microgrid concept - white paper on integration of distributed energy resources," *Technical Report*, U.S. Department of Energy, 2002.

[2] Y. W. Li and C. N. Kao, "An accurate power control strategy for power-electronics-interfaced distributed generation units operating in a low-voltage multibus microgrid," *IEEE Trans. Power Electron.*, vol. 24, no. 12, pp. 2977-2988, 2009.

[3] Q. C. Zhong, "Robust droop controller for accurate proportional load sharing among inverters operated in parallel," *IEEE Trans. Ind. Electron.*, vol. 60, no. 4, pp. 1281-1290, 2013.

[4] C. K. Sao and P. W. Lehn, "Autonomous load sharing of voltage source converters," *IEEE Trans. Power Del.*, vol. 20, no. 2, pp. 1009–1016, 2005.

[5] J. M. Guerrero, J. C. Vasquez, J. Matas, et al, "Hierarchical control of droop-controlled AC and DC microgrids - a general approach toward standardization," *IEEE Trans. Ind. Electron.*, vol. 58, no. 1, pp. 158-172, 2011.

[6] N. Pogaku, M. Prodanović and T. C. Green, "Modeling, analysis and testing of autonomous operation of an inverter-based microgrid," *IEEE Trans. Power Electron.*, vol. 22, no. 2, pp. 613-625, 2007.

[7] X. Lu, J. M. Guerrero, R. Teodorescu, T. Kerekes, et al, "Control of parallel-connected bidirectional AC-DC converters in stationary frame for microgrid application," *in Proc. of IEEE ECCE*, pp. 4153-4160, 2011.

[8] A. Pratt, P. Kumar and T. V. Aldridge, "Evaluation of 400V DC distribution in telco and data centers to improve energy efficiency," *in Proc. of INTELEC*, pp. 32-39, 2007.

[9] H. Kakigano, Y. Miura and T. Ise, "Distribution voltage control for dc microgrids using fuzzy control and gain-scheduling technique," *IEEE Trans. Power Electron.*, vol. 28, no. 5, pp. 2246-2258, 2013.

[10] K. Sun, L. Zhang, Y. Xing and J. M. Guerrero, "A distributed control strategy based on DC bus signaling for modular photovoltaic generation systems with battery energy storage," *IEEE Trans. Power Electron.*, vol. 26, no. 10, pp. 3032-3045, 2011.

[11] X. Lu, J. M. Guerrero, K. Sun and J. C. Vasquez, "An improved droop control method for DC microgrids based on low bandwidth communication with DC bus voltage restoration and enhanced current sharing accuracy," *IEEE Trans. Power Electron.*, vol. 29, no. 4, pp. 1800-1812, 2014.

[12] X. Lu, J. M. Guerrero, K. Sun, J. C. Vasquez, et al, "Hierarchical control of parallel AC-DC converter interfaces for hybrid microgrids," *IEEE Trans. Smart Grid*, vol. 5, no. 2, pp. 683-692, 2014.

[13] D. Dong, I. Cvetkovic, D. Boroyevich, W. Zhang, et al, "Grid-interface bi-directional converter for residential DC distribution systems – part one: high-density two-stage topology," *IEEE Trans. Power Electron.*, vol. 28, no. 4, pp. 1655-1666, 2013.

[14] X. Lu, K. Sun, J. M. Guerrero, J. C. Vasquez and L. Huang, "State-of-charge balance using adaptive droop control for distributed energy storage systems in dc micro-grid applications," *IEEE Trans. Ind. Electron.*, vol. 61, no. 6, pp. 2804-2815, 2014.

[15] J. M. Carrasco, L. G. Franquelo, J. T. Bialasiewicz, et al, "Power-electronic systems for the grid integration of renewable energy sources: a survey," *IEEE Trans. Ind. Electron.*, vol. 53, no. 4, pp. 1002-1016, 2006.

[16] J. Rajagopalan, K. Xing, Y. Guo and F. C. Lee, "Modeling and dynamic analysis of paralleled dc/dc converters with master-slave current sharing control," *in Proc.of APEC*, 1996, pp.678-684.

[17] T. F. Wu, Y. K. Chen and Y. H. Huang, "3C strategy for inverters in parallel operation achieving an equal current distribution," *IEEE Trans. Ind. Electron.*, vol.47, no.2, pp.273-281, 2000.

[18] X. Sun, Y. S. Lee and D. H. Xu, "Modeling, analysis, and implementation of parallel multi-inverter systems with instantaneous average-current-sharing scheme," *IEEE Trans. Power Electron.*, vol.18, no.3, pp. 844-856, 2003.

[19] X. Lu, K. Sun, J. M. Guerrero and L. Huang, "SoC-based dynamic power sharing method with AC-bus voltage restoration for microgrid applications," *in Proc. of IEEE IECON*, pp. 5677-5682, 2012.

[20] International standard for conductors of insulated cables, IEC-60228, 2004.